Inorganic Chemistry

pubs.acs.org/IC

Communication

Superstructural Assembly of Ag_{24} Nanoclusters with Different Ligands Exhibiting Mechanoresponsive Luminescence

Deepak Kumar Patel, Ankit Sharma, Arijit Jana, Jayoti Roy, Amoghavarsha Ramachandra Kini, Vivek Yadav, Subrata Duary, Kumaran Nair Valsala Devi Adarsh,* Sundargopal Ghosh,* and Thalappil Pradeep*

Cite This: https://doi.org/10.1021/acs.inorgchem.6c01760

Read Online

ACCESS | Metrics & More | Article Recommendations | Supporting Information

ABSTRACT: While single thiolate-stabilized silver nanoclusters (NCs) are well studied, multiligand-protected analogues remain rare. Herein, we report a luminescent Ag_{24} nanocluster, co-stabilized by two distinct heterocyclic thiols, 2-mercapto-5-*n*-propylpyrimidine and 6-(dibutylamino)-1,3,5-triazine-2,4-dithiol, together with triphenylphosphine, whose composition was confirmed by high resolution electrospray ionization (HR-ESI) mass spectrometry. It shows aggregation-caused quenching as it self-assembles into nonemissive sheets, but the emission reappears after mechanical grinding, demonstrating mechanoresponsive luminescence. Interestingly, individual ligands form nonluminescent clusters exhibiting no aggregation behavior. Femtosecond transient absorption measurements indicate that aggregation alters the excited-state dynamics, reflecting the effect of multiligand stabilization on structural rigidity and photophysical behavior in the NCs.

Noble metal nanoclusters (NCs), particularly silver NCs, have attracted considerable attention owing to their atomically precise structures and size-dependent photophysical properties arising from quantum confinement effects.[1−4] Their potential applications span across nanoelectronics, catalysis, and bioimaging.[5−7] As unprotected NCs are intrinsically unstable, surface ligands are essential for stabilizing the metal core and tuning their geometric, optical, and electronic properties.[1,6,8] Among the most commonly employed ligands for coinage metal NCs are organothiolates, organophosphines, and alkynyls.[9−11] As the field of nanoclusters has expanded, ligands such as selenolates, amines, and carbene-based ligands have been incorporated, broadening the structural and functional diversity of metal NCs.[12−14]

Heteroaromatic thiols are a distinct yet underexplored class of ligands that can modulate metal−ligand charge transfer and photophysical properties.[15] However, nanoclusters stabilized by multiple ligand types remain rare because of steric and electronic incompatibilities at the cluster surface.[16] Previous studies have predominantly focused on monodentate or thiol systems, leaving a fundamental gap in understanding how heterogeneous ligand-shell environments created by multiple heterocyclic thiols influence nanocluster stability, self-assembly, and stimuli-responsive luminescence.[17−19] In this context, the investigation of mixed-ligand nanoclusters provides an opportunity to explore the relationship between surface chemical complexity, solid-state organization, and luminescent behavior.

The optical properties of NCs are strongly influenced by supramolecular organization through noncovalent interactions, which can induce aggregation-induced emission (AIE) or disaggregation-enhanced emission (DEE) in response to external stimuli.[20,21] For example, ligand dynamics in $Ag_{29}(BDT)_{12}(TPP)_4$ can modulate photoluminescence by up to 13-fold.[22] These studies highlight the critical role of ligand shells in governing nanocluster assembly and photophysical behavior.

Motivated by these observations, we employed a mixed-ligand strategy using triphenylphosphine (TPP), 2-mercapto-5-*n*-propylpyrimidine (HMPP), and 6-(dibutylamino)-1,3,5-triazine-2,4-dithiol (TRZDT) to prepare an Ag_{24} nanocluster. To our knowledge, this is a rare example of a luminescent silver nanocluster co-stabilized by two nitrogen-containing heterocyclic thiols and a phosphine ligand. The pyrimidine and triazine ligands provide multiple coordination sites that strengthen Ag−S bonding and promote intermolecular interactions, while TPP enhances cluster stability through steric and electronic effects.[15,23]

The Ag_{24} nanocluster was synthesized through a mixed-ligand exchange reaction with $[Ag_{18}H_{16}(TPP)_{10}]^{2+}$, following a ligand exchange-induced structural transformation (LEIST) strategy (Figures S1 and S2).[10] Briefly, HMPP (5 mg) and TRZDT (3 mg) dissolved in methanol (2 mL) were added to Ag_{18} NCs (15 mg in 5 mL methanol) under stirring. Color changed from green to purple to yellowish green in 3 h. Post-synthetic size focusing and phase stabilization yielded distinct absorption features at 420, 580, and 620 nm (Figure 1b), indicative of discrete molecular electronic states. Time-dependent UV−vis spectroscopy revealed gradual conversion

Received: April 6, 2026
Revised: June 25, 2026
Accepted: July 2, 2026

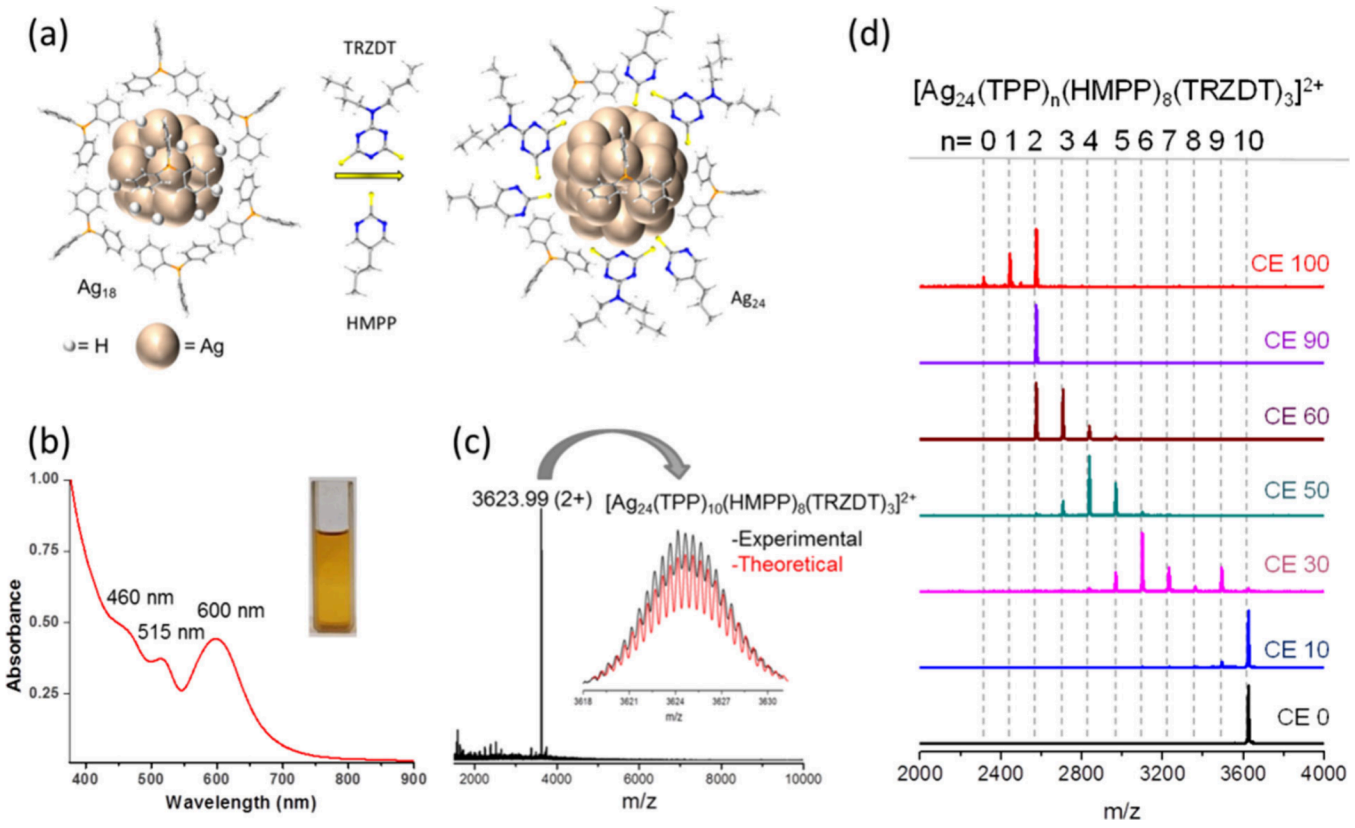

Figure 1. (a) Synthesis of Ag_{24} NC. (b) UV−vis spectrum of Ag_{24} in methanol (inset is a photograph of the solution). (c) HR-ESI mass spectrum with experimental and simulated isotopic patterns. (d) CE-dependent MS/MS fragmentation of the parent ion (m/z 3623.99), showing sequential loss of ten TPP ligands up to CE 100.

of Ag_{18} intermediates to Ag_{24}, with increasing absorbance intensity over time (Figure S2). Despite extensive crystallization trials using various solvents, single crystals suitable for X-ray analysis could not be obtained. Nevertheless, HR-ESI-MS provided unambiguous evidence for the composition $Ag_{24}(TPP)_{10}(HMPP)_8(TRZDT)_3]^{2+}$. The positive-ion mass spectrum displayed a distinct isotopic envelope centered at m/z 3623.99 corresponding to a dicationic species (Figure 1c). The peak-to-peak separation of m/z 0.5 confirmed the 2+ charge state. The total mass of 7247.98 was assigned to $[Ag_{24}(C_{18}H_{15}P)_{10}(C_7H_9N_2S)_8(C_{11}H_{18}N_4S_2)_3]^{2+}$, representing a rare example of a silver cluster stabilized by two distinct thiolate and phosphine ligands. The experimental isotopic pattern closely matched the simulated distribution. Tandem MS/MS experiments performed with increasing collision energy (CE) (Figure 1d) showed sequential loss of ten TPP ligands (262 Da each) from the parent ion at m/z 3623.99 (2+) over the CE range of 0−100, confirming the presence of ten TPP ligands and their labile coordination. Interestingly, use of a single ligand yielded clusters with different nuclearity (Figure S3).[15]

The coexistence of all three capping ligands (TPP, HMPP, and TRZDT) in Ag_{24} was further verified by multinuclear NMR and FT-IR spectroscopy (Figures S6−S9). The ^{1}H NMR spectrum shows a broad aromatic region between 7.1 and 7.7 ppm, arising from coordinated TPP and HMPP ligands. In addition, three well-resolved aliphatic signals at approximately 2.1, 1.3, and 0.8 ppm are assigned to the propyl and butyl chains. The ^{13}C NMR spectrum exhibits aromatic carbon resonances in the range of 128−136 ppm, together with three aliphatic signals at 31.5, 23.6, and 13.5 ppm, consistent with ligand-bound alkyl groups. The ^{31}P NMR spectrum shows a dominant resonance at 7.4 ppm, along with a signal at 29.1 ppm, indicating coordinated TPP with a small contribution from oxidized TPPO. FTIR spectra further confirm incorporation of both thiol ligands into Ag_{24} (Figure S9). The C−H stretching vibrations in the 2950−2850 cm^{-1} region are attributed to the butyl and propyl groups of TRZDT and HMPP. In the free ligands, the C−N and C═N stretching vibrations appear in the 1600−1500 cm^{-1} range; upon formation of Ag_{24}, these bands shift to lower wavenumbers and broaden, reflecting changes in the electronic environment upon coordination to silver. Notably, the S−H stretching features observed for the free ligands are absent in the cluster spectrum, confirming deprotonation and Ag-thiolate bond formation.

XPS measurements further support the multiligand protection of Ag_{24} (Figure S10, Table S1). The C 1s region shows peaks at 284.8, 285.6, and 286.8 eV. The 284.8 eV peak, assigned to adventitious carbon, was used for charge calibration. The aliphatic C−C/C−H carbon atoms from the ligands overlap with the adventitious carbon signal. The higher binding energy components at 285.6 and 286.8 eV are attributed to C−N/C−S environments from the HMPP and TRZDT ligands. The S $2p_{3/2}$ signal at 162.5 eV is characteristic of thiolate sulfur coordinated to silver. The P $2p_{3/2}$ peak appears at 131.5 eV. The Ag 3d region, centered near 367.8 eV, indicates predominantly Ag^0/Ag−S species with a small contribution from Ag(I) (Table S1).

https://doi.org/10.1021/acs.inorgchem.6c01760
Inorg. Chem. XXXX, XXX, XXX−XXX

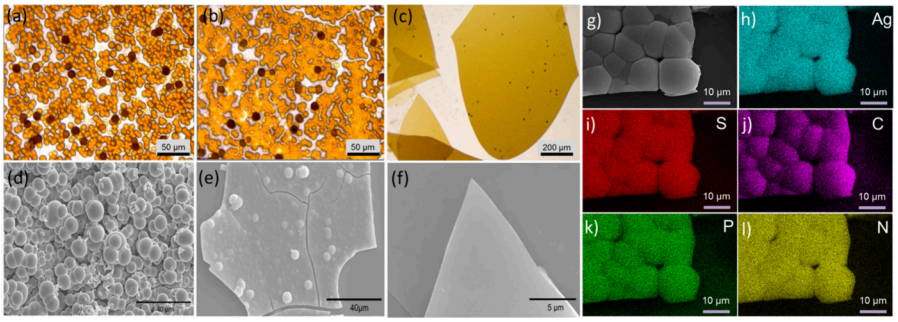

Figure 2. Solvent-induced self-assembly of Ag_{24} clusters. (a–c) Optical images showing microspheres and sheet-like assemblies. (d–f) FESEM images of the corresponding nanostructures. (g–l) EDX mapping of spheroidal assemblies of various elements.

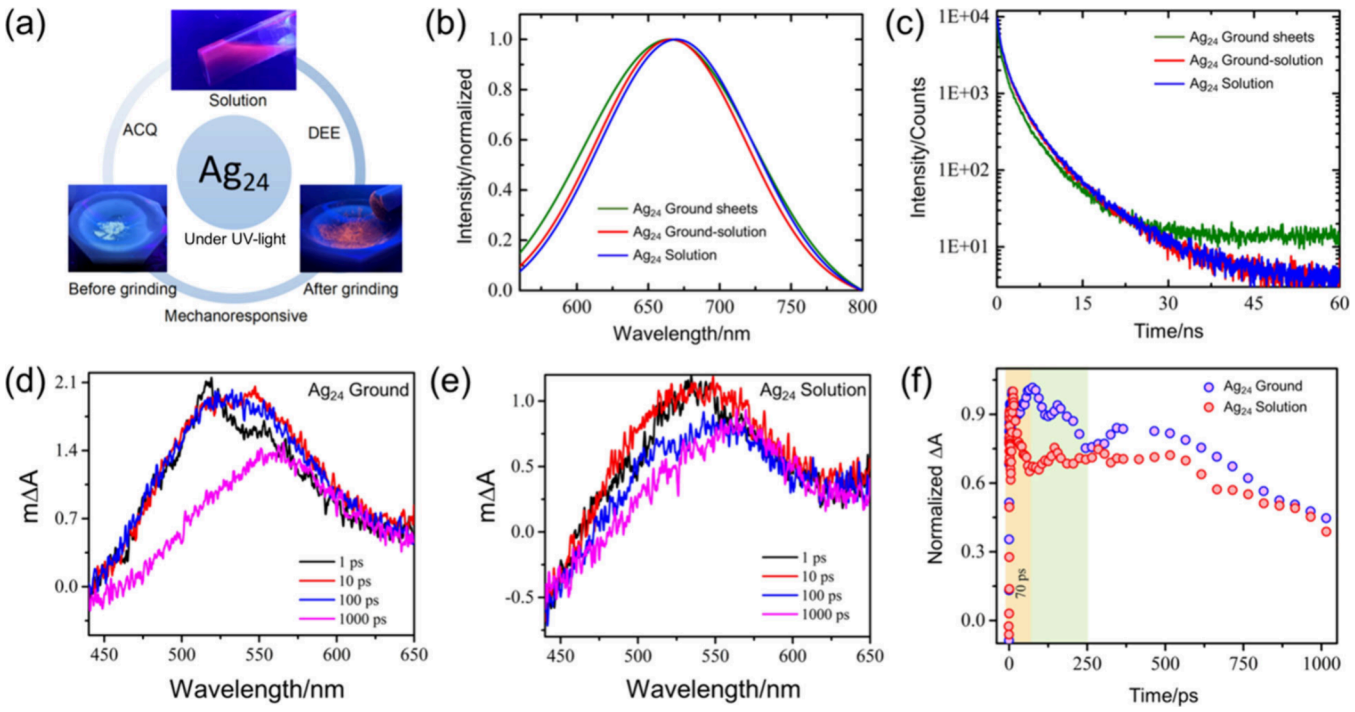

Figure 3. Mechano-responsive luminescence of the Ag_{24}. (a) UV photographs (365 nm) showing emission recovery upon grinding or dissolution of nonemissive aggregates. (b,c) Normalized emission spectra and fluorescence decay profiles of Ag_{24} in DCM solution (blue), ground solid (green), and redissolved sample (red). (d,e) 2D transient absorption maps of the ground and solution-state samples. (f) Transient decay kinetics of the solution and ground samples up to 1 ns.

Interestingly, in a DMF–methanol mixture, Ag_{24} self-assembled into uniform sheet-like aggregates through solvent-mediated organization (Figure 2, Figure S11). The assembly process was controlled by varying cluster concentration and solvent ratios. A mixture of 5 mg Ag_{24} in 1 mL DMF and 0.5 mL methanol yielded spheroidal nanosheets (Figure 2a–c). Keyence digital microscope (VHX-X1 series) and FESEM revealed nearly uniform spheroidal aggregates approximately 500 nm in diameter (see Figure 2d–i, as well as Figures S11 and S12). Similar solvent-driven aggregation has been reported for phosphine-protected Au–Ag alloy NCs.[20] FESEM-EDX analysis reveals elemental compositions (C, N, P, S, and Ag) consistent with the proposed Ag_{24} formulation, confirming retention of the cluster composition in the assembled state (Figure S13). Upon redissolution, UV–vis and ESI-MS recovered the characteristic features of the parent nanocluster without evidence of new stable species (Figure S17). TEM showed particle size below 2 nm, consistent with the atomically precise Ag_{24} core (Figure S14). The assembly is likely driven by hydrophobic interactions among the butyl chains of TRZDT, $\pi\cdots\pi$ stacking between HMPP and TRZDT ligands, and weak N···H hydrogen bonding. These interactions stabilize the spheroidal assemblies, which exhibit aggregation-caused quenching and are nonemissive in the assembled state.

The photophysical properties of Ag_{24} show a strong dependence on supramolecular organization. The as-synthesized nanocluster displays bright red photoluminescence under UV excitation, attributed to ligand-to-metal charge transfer within the Ag-thiolate framework. In contrast, the self-assembled nanosheets are nonemissive (Figure 3a), consistent with aggregation-caused quenching (ACQ) arising from enhanced nonradiative decay pathways in the assembled state.

Mechanical grinding of the aggregated material for approximately 1–2 min restores the emission intensity (Figure 3a). To investigate the associated structural changes, PXRD measurements were performed before and after grinding (Figure S15). The ground sample retains the major diffraction features of the pristine material, although slight peak

https://doi.org/10.1021/acs.inorgchem.6c01760
Inorg. Chem. XXXX, XXX, XXX–XXX

broadening and intensity changes are evident. These observations suggest that the dominant crystalline phase is preserved, while increased structural disorder and/or reduced crystallite size may be introduced. No new diffraction peaks are observed after grinding. The recovery of luminescence is therefore consistent with grinding-induced modifications of intercluster packing and solid-state organization rather than a complete phase transformation. The emission maximum remains unchanged at 665 nm for both the as-synthesized cluster, ground aggregate, and DCM solution via disaggregation-enhanced emission (DEE) (Figure 3b), indicating preservation of the Ag_{24} core structure. The broader emission profile of the ground solid sample is consistent with increased structural heterogeneity and multiple local emissive environments. The PLQY was 2.1% in solution and 1.5% in the ground solid at room temperature, with the solid retaining ~71% of the solution-state emission efficiency.

Time-resolved photoluminescence measurements further elucidate the excited-state dynamics of Ag_{24}. The as-prepared cluster solution exhibited a monoexponential decay with a lifetime of 1.5 ns (Figure 3c). In contrast, the mechanically ground powder displayed a triexponential decay (with τ_1 = 0.204 ± 0.001 ns, τ_2 = 1.14 ± 0.01 ns, and τ_3 = 4.27 ± 0.03 ns). The three relaxation components indicate multiple emissive environments and decay pathways following grinding. The altered decay dynamics are associated with changes in the local environment and intercluster interactions in the solid state. The emergence of longer lifetime component (τ_3 = 4.27 ± 0.03 ns) suggests partial suppression of nonradiative relaxation pathways, resulting in enhanced emission. Similar lifetime enhancement has been reported for $Ag_{29}(BDT)_{12}(TPP)_4$ nanocluster, where restricted structural relaxation improved photoluminescence efficiency.[22]

To gain deeper insight into the mechanoresponsive luminescence behavior, femtosecond transient absorption spectroscopy was performed using a pump−probe technique. Excitation was achieved using 400 nm, 120 fs laser pulses generated via second harmonic generation (BBO crystal) from an 800 nm fundamental wavelength. A fluence of 350 $\mu J/cm^2$ was used to populate higher-energy excited states, while a white-light probe monitored carrier dynamics across the visible region at different time delays. Both as-synthesized and ground Ag_{24} samples exhibited a pronounced photoinduced absorption (PIA) band centered near 530 nm, attributable to excited-state absorption (Figure 3d). The Ag_{24} solution also showed a weak negative transient signal near 620 nm. Because excitation at 400 nm accesses higher-energy electronic states, this feature is assigned to depletion of ground-state population associated with higher-energy optical transitions rather than the lowest-energy transition. This feature was absent in the ground sample (Figure S19), likely due to disruption of intercluster coupling and redistribution of electronic states in the disordered phase. This interpretation is consistent with the red-shift observed in the steady-state absorption of the aggregated samples, indicating a modified electronic environment. Time-dependent analysis of the transient signal at the PIA maximum (~530 nm) reveals clear differences in relaxation behavior (Figure 3e). Within the first ~250 ps, the ground Ag_{24} powder decayed more slowly than the solution sample, suggesting partial suppression of nonradiative relaxation pathways arising from changes in the local environment and intermolecular interactions. At longer delay times, both samples exhibited gradual and incomplete decay within the ~1 ns time window, indicating the presence of long-lived excited states. This slow carrier relaxation likely reflects a triplet-to-singlet transition and nonrelativistic effects in silver clusters.[24]

Longer-time excited-state dynamics were further examined by time-resolved photoluminescence measurements. Upon excitation at 405 nm, both the as prepared and ground-solution samples decayed completely within ~45 ns. In contrast, the ground Ag_{24} solid exhibited an extended decay tail that saturates by ~60 ns. The extended lifetime is possibly due to triplet-to-singlet transition and enhanced rigidity of the ligand shell, which reduces molecular vibration and non-radiative losses.

In summary, we synthesized and characterized a rare luminescent Ag_{24} nanocluster co-stabilized by two distinct nitrogen-containing heterocyclic thiols and a phosphine ligand. Notably, the individual thiol ligands, when employed separately, produce clusters with different nuclearities, highlighting the influence of the mixed-ligand environment on cluster formation. The Ag_{24} exhibits aggregation-caused quenching, disaggregation-enhanced emission, and reversible grinding-induced luminescence recovery. UV−vis, ESI-MS, PXRD, and time-resolved spectroscopic studies indicate that the cluster identity is largely retained during the grinding, while changes in solid-state organization and intercluster interactions govern the luminescence switching behavior. The altered excited-state dynamics of the ground material are consistent with partial suppression of nonradiative relaxation pathways. These findings demonstrate the potential of heteroligand-protected silver nanoclusters for exploring the relationship between surface chemical complexity, supramolecular organization, and stimuli-responsive photophysical properties.

■ ASSOCIATED CONTENT

Supporting Information

The Supporting Information is available free of charge at https://pubs.acs.org/doi/10.1021/acs.inorgchem.6c01760.

Experimental procedures, additional characterization data, spectra, figures, and supplementary discussion (PDF)

■ AUTHOR INFORMATION

Corresponding Authors

Kumaran Nair Valsala Devi Adarsh − *Department of Physics, Indian Institute of Science Education and Research Bhopal, Bhopal 462066, India;* orcid.org/0000-0002-6337-6545; Email: adarsh@iiserb.ac.in

Sundargopal Ghosh − *DST Unit of Nanoscience (DST UNS) and Thematic Unit of Excellence (TUE), Department of Chemistry, IIT Madras, Chennai 600036, India;* orcid.org/0000-0001-6089-8244; Email: sghosh@iitm.ac.in

Thalappil Pradeep − *DST Unit of Nanoscience (DST UNS) and Thematic Unit of Excellence (TUE), Department of Chemistry, IIT Madras, Chennai 600036, India;* orcid.org/0000-0003-3174-534X; Email: pradeep@iitm.ac.in

Authors

Deepak Kumar Patel − *DST Unit of Nanoscience (DST UNS) and Thematic Unit of Excellence (TUE), Department of Chemistry, IIT Madras, Chennai 600036, India;* orcid.org/0000-0003-2509-4165

https://doi.org/10.1021/acs.inorgchem.6c01760
Inorg. Chem. XXXX, XXX, XXX−XXX

Ankit Sharma − *Department of Physics, Indian Institute of Science Education and Research Bhopal, Bhopal 462066, India; Department of Physics and Astronomy, Aarhus University, DK-8000 Aarhus C, Denmark;* orcid.org/0009-0005-0395-0858

Arijit Jana − *DST Unit of Nanoscience (DST UNS) and Thematic Unit of Excellence (TUE), Department of Chemistry, IIT Madras, Chennai 600036, India;* orcid.org/0000-0002-5676-0688

Jayoti Roy − *DST Unit of Nanoscience (DST UNS) and Thematic Unit of Excellence (TUE), Department of Chemistry, IIT Madras, Chennai 600036, India;* orcid.org/0009-0006-6535-0011

Amoghavarsha Ramachandra Kini − *DST Unit of Nanoscience (DST UNS) and Thematic Unit of Excellence (TUE), Department of Chemistry, IIT Madras, Chennai 600036, India;* orcid.org/0009-0003-6863-7729

Vivek Yadav − *DST Unit of Nanoscience (DST UNS) and Thematic Unit of Excellence (TUE), Department of Chemistry, IIT Madras, Chennai 600036, India;* orcid.org/0009-0004-0244-0541

Subrata Duary − *DST Unit of Nanoscience (DST UNS) and Thematic Unit of Excellence (TUE), Department of Chemistry, IIT Madras, Chennai 600036, India*

Complete contact information is available at: https://pubs.acs.org/10.1021/acs.inorgchem.6c01760

Author Contributions

D.K.P. carried out the experimental synthesis, characterization, and data analysis. A.J., V.Y., and SD helped during the synthesis. A.S. and K.V.A. conducted the luminescence study and femtosecond transient absorption spectroscopy. A.R.K. performed the XPS analysis. D.K.P. prepared the first draft of the manuscript, and all authors contributed to revising and finalizing the manuscript. S.G. and T.P. supervised the project.

Notes

The authors declare no competing financial interest.

■ ACKNOWLEDGMENTS

D.K.P. acknowledges the PMRF for fellowship. T.P. thanks SERB for funding through Grant No. SPR/2021/000439 and a JC Bose Fellowship. We thank the support from the CoE on Molecular Materials and Functions under the Institute of Eminence scheme of IIT Madras. We thank Ms. Celin Rooth for performing PLQY measurements.

■ REFERENCES

(1) Chakraborty, I.; Pradeep, T. Atomically Precise Clusters of Noble Metals: Emerging Link between Atoms and Nanoparticles. *Chem. Rev.* **2017**, *117* (12), 8208−8271.

(2) Jin, R.; Zeng, C.; Zhou, M.; Chen, Y. Atomically Precise Colloidal Metal Nanoclusters and Nanoparticles: Fundamentals and Opportunities. *Chem. Rev.* **2016**, *116* (18), 10346−10413.

(3) Higaki, T.; Li, Q.; Zhou, M.; Zhao, S.; Li, Y.; Li, S.; Jin, R. Toward the Tailoring Chemistry of Metal Nanoclusters for Enhancing Functionalities. *Acc. Chem. Res.* **2018**, *51* (11), 2764−2773.

(4) Jose, A.; Sooraj, B. S.; Pradeep, T. Precision at the Nanoscale: An 'Ionic' View of Composition, Structure and Properties. *Nanoscale* **2026**, *18* (1), 15−65.

(5) Chen, L.; Black, A.; Parak, W. J.; Klinke, C.; Chakraborty, I. Metal Nanocluster-based Devices: Challenges and Opportunities: Nanoscience: Special Issue Dedicated to Professor Paul S. Weiss. *Aggregate* **2022**, *3* (4), No. e132.

(6) Jin, R.; Li, G.; Sharma, S.; Li, Y.; Du, X. Toward Active-Site Tailoring in Heterogeneous Catalysis by Atomically Precise Metal Nanoclusters with Crystallographic Structures. *Chem. Rev.* **2021**, *121* (2), 567−648.

(7) Fan, C.; Lv, X.; Liu, F.; Feng, L.; Liu, M.; Cai, Y.; Liu, H.; Wang, J.; Yang, Y.; Wang, H. Silver Nanoclusters Encapsulated into Metal−Organic Frameworks with Enhanced Fluorescence and Specific Ion Accumulation toward the Microdot Array-Based Fluorimetric Analysis of Copper in Blood. *ACS Sens.* **2018**, *3* (2), 441−450.

(8) Jash, M.; Methikkalam, R. R. J.; Bodiuzzaman, M.; Paramasivam, G.; Pradeep, T. Reaction between Ag_{17}^{+} and Acetylene Outside the Mass Spectrometer: Dehydrogenation in the Gas Phase. *Chem. Commun.* **2020**, *56* (100), 15623−15626.

(9) Desireddy, A.; Conn, B. E.; Guo, J.; Yoon, B.; Barnett, R. N.; Monahan, B. M.; Kirschbaum, K.; Griffith, W. P.; Whetten, R. L.; Landman, U.; Bigioni, T. P. Ultrastable Silver Nanoparticles. *Nature* **2013**, *501* (7467), 399−402.

(10) Bootharaju, M. S.; Dey, R.; Gevers, L. E.; Hedhili, M. N.; Basset, J.-M.; Bakr, O. M. A New Class of Atomically Precise, Hydride-Rich Silver Nanoclusters Co-Protected by Phosphines. *J. Am. Chem. Soc.* **2016**, *138* (42), 13770−13773.

(11) Lei, Z.; Wan, X.-K.; Yuan, S.-F.; Guan, Z.-J.; Wang, Q.-M. Alkynyl Approach toward the Protection of Metal Nanoclusters. *Acc. Chem. Res.* **2018**, *51* (10), 2465−2474.

(12) Chakraborty, I.; Kurashige, W.; Kanehira, K.; Gell, L.; Häkkinen, H.; Negishi, Y.; Pradeep, T. Ag_{44} $(SeR)_{30}$: A Hollow Cage Silver Cluster with Selenolate Protection. *J. Phys. Chem. Lett.* **2013**, *4* (19), 3351−3355.

(13) Jana, A.; Chakraborty, P.; Dar, W. A.; Chandra, S.; Khatun, E.; Kannan, M. P.; Ras, R. H. A.; Pradeep, T. Dual Emitting Ag_{35} Nanocluster Protected by 2-Pyrene Imine Thiol. *Chem. Commun.* **2020**, *56* (83), 12550−12553.

(14) Yi, H.; Osten, K. M.; Levchenko, T. I.; Veinot, A. J.; Aramaki, Y.; Ooi, T.; Nambo, M.; Crudden, C. M. Synthesis and Enantioseparation of Chiral Au_{13} Nanoclusters Protected by Bis- *N* -Heterocyclic Carbene Ligands. *Chem. Sci.* **2021**, *12* (31), 10436−10440.

(15) Jana, A.; Dar, W. A.; Jana, S. K.; Poonia, A. K.; Yadav, V.; Roy, J.; Chandra, S.; Adarsh, K. N. V. D.; Ras, R. H. A.; Pradeep, T. Photoconversion of Ag_{31} to Ag_{42} Initiated by Solvated Electrons. *Chem. Mater.* **2023**, *35* (17), 7020−7031.

(16) Wang, X.-J.; Langetepe, T.; Persau, C.; Kang, B.-S.; Sheldrick, G. M.; Fenske, D. Syntheses and Crystal Structures of the New Ag−S Clusters [Ag70S16(SPh)34(PhCO2)4(Triphos)4] and [Ag188S94-(PR3)30]. *Angew. Chem., Int. Ed.* **2002**, *41* (20), 3818−3822.

(17) Som, A.; Griffo, A.; Chakraborty, I.; Hähl, H.; Mondal, B.; Chakraborty, A.; Jacobs, K.; Laaksonen, P.; Ikkala, O.; Pradeep, T.; Nonappa. Strong and Elastic Membranes via Hydrogen Bonding Directed Self-Assembly of Atomically Precise Nanoclusters. *Small* **2022**, *18* (34), No. 2201707.

(18) Sagara, Y.; Yamane, S.; Mitani, M.; Weder, C.; Kato, T. Mechanoresponsive Luminescent Molecular Assemblies: An Emerging Class of Materials. *Adv. Mater.* **2016**, *28* (6), 1073−1095.

(19) Sugi, K. S.; Sandra, A. P.; Nonappa; Ghosh, D.; Mohanty, J. S.; Paulthangam Kannan, M.; Sooraj, B. S.; Srikrishnarka, P.; Roy, J.; Dar, W. A.; Pradeep, T. Secondary Ligand-Induced Orthogonal Self-Assembly of Silver Nanoclusters into Superstructures with Enhanced NIR Emission. *Nanoscale* **2023**, *15* (28), 11927−11934.

(20) Jash, M.; Jana, A.; Poonia, A. K.; Khatun, E.; Chakraborty, P.; Nagar, A.; Ahuja, T.; Adarsh, K. V.; Pradeep, T. Phosphine-Protected Atomically Precise Silver−Gold Alloy Nanoclusters and Their Luminescent Superstructures. *Chem. Mater.* **2023**, *35* (1), 313−326.

(21) Duary, S.; Jana, A.; Das, A.; Acharya, S.; Kini, A. R.; Roy, J.; Poonia, A. K.; Patel, D. K.; Yadav, V.; Antharjanam, P. K. S.; Pathak, B.; Kumaran Nair Valsala Devi, A.; Pradeep, T. Milling-Induced "Turn-off" Luminescence in Copper Nanoclusters. *Inorg. Chem.* **2024**, *63* (40), 18727−18737.

(22) Kang, X.; Wang, S.; Zhu, M. Observation of a New Type of Aggregation-Induced Emission in Nanoclusters. *Chem. Sci.* **2018**, *9* (11), 3062−3068.
(23) Mishra, D.; Wang, S.; Jin, Z.; Xin, Y.; Lochner, E.; Mattoussi, H. Highly Fluorescent Hybrid Au/Ag Nanoclusters Stabilized with Poly(Ethylene Glycol)- and Zwitterion-Modified Thiolate Ligands. *Phys. Chem. Chem. Phys.* **2019**, *21* (38), 21317−21328.
(24) Yadav, V.; Jana, A.; Acharya, S.; Malola, S.; Nagar, H.; Sharma, A.; Kini, A. R.; Antharjanam, S.; Machacek, J.; Adarsh, K. N. V. D.; Base, T.; Häkkinen, H.; Pradeep, T. Site-Specific Substitution in Atomically Precise Carboranethiol-Protected Nanoclusters and Concomitant Changes in Electronic Properties. *Nat. Commun.* **2025**, *16* (1), 1197.

https://doi.org/10.1021/acs.inorgchem.6c01760
Inorg. Chem. XXXX, XXX, XXX−XXX